New Phytologist

Research

Divergent hydraulic strategies to cope with freezing in co-occurring temperate tree species with special reference to root and stem pressure generation

Xiao-Han Yin[1,2], Frank Sterck[3] and Guang-You Hao[1]

[1]CAS Key Laboratory of Forest Ecology and Management, Institute of Applied Ecology, Chinese Academy of Sciences, Shenyang 110016, China; [2]College of Resources and Environment, University of Chinese Academy of Sciences, Beijing 100049, China; [3]Forest Ecology and Forest Management Group, Wageningen University, PO Box 47, 6700 AA Wageningen, the Netherlands

Author for correspondence:
Guang-You Hao
Tel: +86 24 8397 0374
Email: haogy@iae.ac.cn

Received: *27 November 2017*
Accepted: *18 March 2018*

New Phytologist (2018)
doi: 10.1111/nph.15170

Key words: cavitation, freeze–thaw cycle, frost fatigue, root pressure, temperate forest, xylem hydraulics.

Summary

- Some temperate tree species mitigate the negative impacts of frost-induced xylem cavitation by restoring impaired hydraulic function via positive pressures, and may therefore be more resistant to frost fatigue (the phenomenon that post-freezing xylem becomes more susceptible to hydraulic dysfunction) than nonpressure-generating species. We test this hypothesis and investigate underlying anatomical/physiological mechanisms.
- Using a common garden experiment, we studied key hydraulic traits and detailed xylem anatomical characteristics of 18 sympatric tree species. These species belong to three functional groups, that is, one generating both root and stem pressures (RSP), one generating only root pressure (RP), and one unable to generate such pressures (NP).
- The three functional groups diverged substantially in hydraulic efficiency, resistance to drought-induced cavitation, and frost fatigue resistance. Most notably, RSP and RP were more resistant to frost fatigue than NP, but this was at the cost of reduced hydraulic conductivity for RSP and reduced resistance to drought-induced cavitation for RP.
- Our results show that, in environments with strong frost stress: these groups diverge in hydraulic functioning following multiple trade-offs between hydraulic efficiency, resistance to drought and resistance to frost fatigue; and how differences in anatomical characteristics drive such divergence across species.

Introduction

In humid temperate forests, freeze–thaw cycles pose a principal threat to the hydraulic safety of overwintering organs in woody species by inducing embolisms in xylem conduits (Tyree & Sperry, 1989; Pockman & Sperry, 1996; Choat *et al.*, 2011; Granda *et al.*, 2014). Due to the insolubility of gases in ice, gas bubbles are formed when the sap in xylem conduits freezes (Mayr *et al.*, 2002; Pittermann & Sperry, 2006). Upon thawing and recovery of tension in the water columns, bubbles larger than a critical size will grow under the tension and cause embolism (Sperry & Sullivan, 1992; Davis *et al.*, 1999; Lemoine *et al.*, 1999; Mayr *et al.*, 2002; Charra-Vaskou *et al.*, 2016). Larger bubbles are more likely to form in larger xylem conduits and thus species with larger conduits are more prone to freezing-induced embolism (Sperry & Sullivan, 1992; Davis *et al.*, 1999; Pittermann & Sperry, 2006). Even though winter embolism has limited consequences during the dormant season, it can have severe negative effects on plant performance during the subsequent growing season if the hydraulic transport function cannot be restored (Schreiber *et al.*, 2013; Christensen-Dalsgaard & Tyree, 2014). Compared with extensive studies on drought-induced xylem embolism, still relatively few studies have been conducted on xylem hydraulics in relation to frost-induced embolism.

Temperate hardwood (angiosperm) tree species have adopted different strategies to cope with freezing-induced embolism. Ring-porous species with large earlywood vessels have adopted the 'throw away' strategy (Cochard & Tyree, 1990; Sperry *et al.*, 1994; Hacke & Sperry, 2001). They largely lose the xylem hydraulic functionality in winter, but recover this functionality via the production of new early wood in spring, at the onset of the following growing season (Cochard & Tyree, 1990; Sperry *et al.*, 1994; Hacke & Sauter, 1996). By contrast, many diffuse-porous species have adopted the 'avoidance' strategy, as they rely on their smaller conduits that are more resistant to freezing-induced embolism (Sperry & Sullivan, 1992; Hacke & Sperry, 2001). Alternatively, some diffuse-porous species have adopted a 'refilling' strategy, that is, they generate a positive xylem pressure in late winter and/or early spring, and thus refill winter-embolized vessels and restore hydraulic functionality before the start of the growing season (Tibbetts & Ewers, 2000; Hacke & Sperry, 2001; Améglio *et al.*, 2002; Hao *et al.*, 2013b). For

example, root pressure is well-known as an effective mechanism for refilling winter-embolized vessels in *Betula* species (e.g. Sperry *et al.*, 1994; Hao *et al.*, 2013b), whereas positive pressure generated in the stem contributes to refilling of winter-embolized vessels in *Acer* and *Juglans* species (Tyree, 1983; Sperry *et al.*, 1988b; Tyree & Yang, 1992; Améglio *et al.*, 2004). In contrast to nonpressure-generating species, the vulnerability to frost-induced xylem embolism is decoupled from vessel diameters in tree species that generate positive xylem pressures (Niu *et al.*, 2017). Yet, differences in hydraulic performance between pressure-generating species and nonpressure-generating species are poorly studied, and the anatomical and physiological mechanisms underlying those differences require further investigation.

Great divergences in xylem structural characteristics have been observed in temperate tree species, which reflect trade-offs along the 'spectrum' of xylem structure and function variations (Chave *et al.*, 2009; Reich, 2014; Niu *et al.*, 2017). Some tree species can achieve exceptionally high xylem hydraulic efficiency by producing large conduits in earlywood (Christman *et al.*, 2012; Kitin & Funada, 2016; Niu *et al.*, 2017), which is due to the fact that theoretical hydraulic conductivity of a conduit is proportional to the fourth power of its diameter according to the Hagen–Poiseuille law (Zimmermann, 1983). However, large vessel sizes of these tree species make them unavoidably more vulnerable to freezing-induced loss of hydraulic conductivity due to the strong positive correlation between vessel size and vulnerability to freezing-induced embolism (Feild & Brodribb, 2001; Jiménez-Castillo & Lusk, 2013). Some other tree species reduce the risk of freezing-induced embolism by producing conduits of small sizes, but this comes at the cost of a lower hydraulic efficiency (Hacke & Sperry, 2001; Lens *et al.*, 2013; Niu *et al.*, 2017). Besides the influence of tissue-level xylem characteristics, hydraulic efficiency and safety of xylem also are strongly affected by pit anatomical traits. It has been shown that resistance to water flow through intervessel pits accounts for a high proportion (often > 50%) of the total xylem hydraulic resistance (Wheeler *et al.*, 2005; Lens *et al.*, 2011; Christman *et al.*, 2012). Pit characteristics favoring a higher water permeability (e.g. larger pit membrane area and pit aperture) are often at the cost of reduced resistance to drought-induced cavitation and vice versa (Hacke & Sperry, 2001; Christman *et al.*, 2012; Lens *et al.*, 2013; Zhang *et al.*, 2017). How such vessel and pit characteristics are coupled to the ability (or inability) of tree species to generate positive xylem pressure and their recovery from frost-induced embolism is poorly understood. This study aims at filling this gap in our knowledge.

Although the hydraulic function of winter-embolized xylem can be refilled using positive xylem pressure, some irreversible structural damages may occur to the conduit cell walls during the process of embolism formation that reduce the cavitation resistance of the conduits after thawing. This phenomenon is termed as 'frost fatigue' by analogy with 'cavitation fatigue', which is the increase in xylem susceptibility to drought-induced cavitation in stems that went through a cavitation-refilling process (Stiller & Sperry, 2002; Christensen-Dalsgaard & Tyree, 2013). During the process of drought-induced xylem cavitation, the cellulose microfibrils at the air–sap interfaces can be stretched and deformed, resulting in the loosening of the pit membrane meshes (Hacke *et al.*, 2001b; Jacobsen *et al.*, 2005; Christensen-Dalsgaard & Tyree, 2013). Even if these vessels can be refilled, these structural damages to pit membrane may result in reduced resistance to hydraulic dysfunction when plants are facing drought stresses again. Likewise, frost fatigue is quantified by how much the hydraulic vulnerability curve is shifted after freezing/thawing induced embolism and refilling, and is typically reported as a shift in the xylem water potential corresponding to 50% loss of hydraulic conductivity (P_{50}) (Hacke *et al.*, 2001b; Feng *et al.*, 2015). For example, P_{50} was reduced by 87% and vulnerability curves changed from s-shaped to r-shaped in a *Populus* species through the winter (Christensen-Dalsgaard & Tyree, 2014), which would seriously affect the hydraulic safety of the post-frost trees (Hacke *et al.*, 2001b). Frost fatigue is likely to be a major threat to the hydraulic functioning of temperate trees exposed to frequent freeze–thaw cycles and characteristics related to frost fatigue may have great adaptive significance (Christensen-Dalsgaard & Tyree, 2013), but it is still poorly understood due to the scarcity of empirical studies.

Greater resistance to frost fatigue and its associated xylem structural characteristics was likely selected in tree species being able to refill winter-embolized vessels using positive pressure, considering the fact that vessels need to be used for multiple years in these species (Christensen-Dalsgaard & Tyree, 2014), but this hypothesis has not yet been tested. In the present study, we quantified frost fatigue resistance and a suite of hydraulics-related xylem anatomical characters at the tissue and pit levels in sympatric temperate tree species that differ in their strategies of coping with winter embolism: that is, species that can generate both root and stem pressures (RSP), species that can generate root pressure only (RP), and species that do not generate positive xylem pressure (NP). The RSP and RP species were separated in the present study because these species groups differ in mechanisms of pressure generation (Tyree, 1983; Johnson *et al.*, 1987; Sperry *et al.*, 1987; Sperry, 1993; Cirelli *et al.*, 2008), as well as in their habitat preferences and dominance in the forests where they co-occur. We tested the following three specific hypotheses: species groups with stronger ability to refill winter-embolized vessels have greater resistance to frost fatigue (i.e. ranking this resistance from high to low: RSP > RP > NP); species groups differ in xylem anatomical characteristics at both the tissue and pit levels, reflecting their differences in frost fatigue resistance; and divergence in these xylem anatomical characteristics causes trade-offs between frost-fatigue resistance, hydraulic efficiency and hydraulic safety across species groups. To test these hypotheses, cavitation vulnerability curves were fitted between measured values of percentage loss of conductivity (PLC) using the Cavitron method (Cochard *et al.*, 2005) in stems with and without a controlled freeze–thaw cycle treatment in 18 sympatric tree species that were classified into the three abovementioned functional groups (Table 1). Xylem anatomical characteristics related to hydraulic efficiency and safety at both the tissue and pit levels were analyzed in detail to investigate the structural basis underlying the potential hydraulic differences among functional groups.

Table 1 List of the 18 studied tree species belonging to the three different functional groups

Group code	Species	Species code	Symbol	Family	Maximum height (m)
RSP	*Acer barbinerve* Maxim.	*Ab*	●	Aceraceae	10
RSP	*Acer ginnala* Maxim.	*Ag*	▼	Aceraceae	15
RSP	*Acer mandshuricum* Maxim.	*Ama*	▲	Aceraceae	20
RSP	*Acer mono* Maxim.	*Amo*	◆	Aceraceae	20
RSP	*Acer pseudo-sieboldianum* Kom.	*Ap*	■	Aceraceae	15
RSP	*Acer tegmentosum* Maxim.	*At*	⬢	Aceraceae	20
RP	*Alnus japonica* (Thunb.) Steud.	*Aj*	●	Betulaceae	25
RP	*Betula costata* Trautv.	*Bc*	▽	Betulaceae	25
RP	*Betula dahurica* Pall.	*Bd*	△	Betulaceae	25
RP	*Betula fruticosa* Pall.	*Bf*	◇	Betulaceae	20
RP	*Betula platyphylla* Suk.	*Bp*	□	Betulaceae	25
RP	*Betula schmidtii* Regel.	*Bs*	⬡	Betulaceae	20
NP	*Populus davidiana* Dode.	*Pd*	○	Salicaceae	25
NP	*Populus koreana* Rehd.	*Pk*	▽	Salicaceae	25
NP	*Populus pseudo-simonii* Kitag.	*Pp*	△	Salicaceae	25
NP	*Populus ussuriensis* Kom.	*Pu*	◇	Salicaceae	25
NP	*Tilia amurensis* Rupr.	*Ta*	□	Tiliaceae	25
NP	*Tilia mandshurica* Rupr.er Maxim.	*Tm*	⬡	Tiliaceae	25

RSP, species that can generate both stem and root pressures; RP, species that can only generate root pressure; NP, species not being able to generate positive xylem pressure.

Materials and Methods

Study site and plant materials

The study was carried out at the Northeast Asia Botanical Garden (128°28′E, 42°24′N; 736 m altitude), located right next to the Changbai Mountain Nature Reserve, Jilin province, NE China. In this site, the climate is strongly influenced by the monsoon. The mean annual precipitation is *c.* 695 mm and almost 80% falls during the growing season (May to September). The region has a typical temperate continental climate with long, cold winters with 117–158 d of snow cover per year (October–March). There are nearly 100 d per year that the air temperature fluctuates above and below 0°C that can potentially induce freeze-thaw cycles in plant tissues (Niu *et al.*, 2017). The mean annual temperature is 3.3°C. January is the coldest month with a temperature mean of −16.1°C and July is the warmest month with a mean of 19.3°C. The typical climax vegetation in this region is composed of broadleaved deciduous tree species mixed with *Pinus koraiensis* Sieb. et Zucc. This type of vegetation is well-known for its high species richness among temperate forests (Hao *et al.*, 2008b). The common garden set-up guaranteed that the environmental effects on the variation in functional traits across species were minimized, and that interspecific differences reflected genetic differences.

For the present investigation, 18 diffuse-porous tree species co-occurring in a typical forest of this region were selected. The tree species are classified in equal numbers into the three above-mentioned groups: species that can generate both root and stem pressures (RSP), species that can generate root pressure only (RP), and species that do not generate positive xylem pressure (NP). Because the positive-pressure-generating tree species of this region predominantly have diffuse-porous wood (Niu *et al.*, 2017), we also chose diffuse-porous species for the NP group for comparative purpose. Moreover, by only using diffuse-porous tree species we can avoid the potential problem of unrealistically high vulnerability to cavitation when measuring stems with long vessels using the Cavitron method (Cochard *et al.*, 2010). The RSP diffuse-porous tree species belong exclusively to the genus *Acer*, and the RP species belong to *Alnus* and *Betula* (both Betulaceae). Almost all positive pressure-generating species of the region were included in the present study. The generation of stem pressure in *Acer* species, well known as the driving force for maple exudation, differs in mechanism from the more commonly found root pressure (Tyree, 1983; Johnson *et al.*, 1987; Cirelli *et al.*, 2008). Besides the ability of generating stem pressure, *Acer* species can also generate root pressure but in a later season (Sperry *et al.*, 1988b; Ewers *et al.*, 2001). Positive xylem pressures were confirmed in these species in late winter and/or early spring by clipping off small branches and observing sap exudation from the wounds. For the NP group, we selected species from two genera that have the highest dominance in the native forest of this region, that is, four *Populus* species (Salicaceae) and two *Tilia* species (Tiliaceae). Only trees of mature size were sampled for all species.

Hydraulic conductivity, vulnerability curves and frost fatigue

For measuring maximum stem hydraulic conductivity (K_{max}) and constructing hydraulic vulnerability curves (VCs), six 1-m-long branches were collected from different individuals of each species in August 2016. A stem segment of *c.* 50 cm in length was excised under water immediately after a branch was cut from the tree. Samples were transported to the laboratory while kept under water in an incubator. In the laboratory, the samples were stored at 4°C in a refrigerator while kept under water before hydraulic measurements. All hydraulic measurements were done within 3 d of sampling. Measurements of K_{max}, and the construction of VCs were performed using a modified 'Cochard Cavitron' system,

which measures hydraulic conductivity while the stem is spinning under adjustable speeds (Cai & Tyree, 2010). Briefly, a stem segment was placed in the rotor mounted on a centrifuge with both ends of the segment placed in cuvettes filled with 20 mM KCl solution. The pressure difference, generated by the different height of liquid in the cuvettes during spinning, drove water flow through the stem segment and the hydraulic conductivity was calculated by measuring the dynamic changes of the volume of water remaining in the cuvette.

Before the measurements, a stem segment of 27.4 cm in length was sampled underwater from the middle part of the originally sampled 50-cm-long segment. After shaving both ends using a sharp razor blade, it was connected to a tubing apparatus and flushed with filtered (0.2 μm) 20 mM KCl solution at 100 kPa for 15 min to eliminate native embolisms before it was fitted into the centrifuge rotor. The K_{max} was measured while the segment was spinning at 153 ***g*** (causing a tension of 0.088 MPa in the xylem), assuming that this small tension was too small to cause any cavitation. The hydraulic conductivity was allowed to stabilize for 15 min while the segment was spinning at 153 ***g*** before K_{max} was recorded (Feng *et al.*, 2015). The segment was then subjected to stepwise increases in spin speeds at 0.3 MPa intervals of the resulted xylem tension and the hydraulic conductivity (K_h) was measured at each spin speed allowing a stabilization time of 3 min. The PLC was calculated as $100(1 - K_h/K_{max})$. The spin speed was eventually increased until there was no further measurable hydraulic conductivity. Vulnerability curves were fitted using a Weibull function (Cai & Tyree, 2010):

$$\mathrm{PLC} = 100 \times \left(1 - \exp\left(-\frac{T^c}{b}\right)\right.$$

The P_{50} was determined for each stem by a best-fit Weibull function from the vulnerability curve. Maximum specific hydraulic conductivity (K_s, kg m^{-1} s^{-1} MPa^{-1}) was calculated as K_{max} divided by the cross-sectional sapwood area of the segment (Sperry *et al.*, 1988a). The cross-sectional sapwood area was calculated by measuring the diameter of the stem (bark removed) with a digital caliper (no obvious pith and heartwood was found in stem samples of all the studied species). The same set of stem segments were used for wood density (WD) measurements using the water displacement method.

For determining the resistance to frost fatigue, three pairs of branches (with each pair collected from the same individual) were sampled for each species during the growing season. Three segments, each from a different pair, were first treated with an experimentally controlled freeze–thaw cycle before the determination of VCs. VCs were determined directly (without the freeze–thaw treatment) in the other three segments. For the freeze–thaw cycle treatment, stem segments were frozen and thawed while spinning in a superspeed cyro centrifuge (Model 20K, Cence Instruments, Changsha, China) equipped with a customized 'Sperry type' rotor at 506 ***g***, that is, creating a known tension of 0.3 MPa. During this treatment, stems were exposed to freezing temperature for 8 h at −7°C while spinning. The stems were thawed to room temperature under the same tension generated by the centrifuge that took *c.* 40 min. Both the freeze–thaw-treated segments and the control segments were flushed for 15 min under a 100 kPa pressure with 20 mM KCl solution before the determination of the VCs using the abovementioned Cavitron system. The resistance to frost fatigue was quantified as P_{50} of the control segment minus that of the treated segment (ΔP_{50}) in each pair.

Light microscopy

Stem transverse sections measuring 20 μm thick from six segments (0.8–1.0 cm in diameter) per species were prepared using a sliding microtome (Model 2010-17; Shanghai Medical Instrument Corp., Shanghai, China). Transverse sections were stained with 0.1% toluidine blue to increase visual contrasts. The transverse sections were then examined under a light microscope (Leica ICC50, Wetzlar, Germany) and images were taken under magnifications of ×40 with an inbuilt digital camera. Images were taken for three sectors spanning the current and previous growth rings on six cross-sections each from a different individual, resulting in at least 18 images per species. Anatomical characteristics were calculated with the image analysis program ImageJ (US National Institutes of Health, Bethesda, MD, USA). Vessel density (VD, no. mm^{-2}) was determined as the number of vessels per xylem area. Solitary vessel index (V_s) was determined as the number of solitary vessels divided by the total number of vessels in each image. Mean vessel diameter (D) of a species was estimated based on measurements of lumen areas of all vessels appearing in the analyzed images, assuming a circular shape of all the vessels.

Scanning electron microscopy

For measuring xylem anatomical characteristics at the pit level, fresh stem segments with diameters of *c.* 1 cm were cut into 1.5-cm-long segments. After removal of the bark, tangential sections measuring 25 μm thick were made with a sliding microtome (Model 2010-17; Shanghai Medical Instrument Corp.). Tangential sections were subsequently dehydrated gradually through an ethanol series (30–50–70–90%) for 10 min in each solution, immersed in 100% ethanol for 12 h, and finally air-dried. Dried samples were fixed on aluminum stubs using electron conductive carbon cement (Leit-C, Neubauer Chemikalien, Münster, Germany) and sputter-coated with platinum for 2 min at 10 mA in a sputter coater (Quorum SC7620; Quorum Technologies Ltd, East Sussex, UK). Samples were examined using an environmental scanning electron microscope (Quanta™250; FEI Co., Hillsboro, OR, USA) at an accelerating voltage of 20 kV. Pictures were taken under ×10 000 magnifications for calculating pit-level anatomical parameters using ImageJ software. Pit-field fraction (F_{pf}) and the sum of aperture area on per unit intervessel wall area (A_{ap}) were measured on at least 20 different visual fields in six segments per species. Single pit membrane area (A_p), the length ratio of the shortest to longest axis of the pit aperture (AP_f) and aperture fraction (F_{ap}, pit aperture area divided by membrane area) were measured on 100 individual pits from six different individual trees per species.

Statistical analysis

One-way ANOVA was used to test for trait differences between functional groups using mean values for each individual species. We used Pearson's correlation analysis to test for correlations between K_s, P_{50}, ΔP_{50} and the wood anatomical characteristics. Before the statistical analyses, all of the data were tested for normality and equal variance. Principal components analysis (PCA) was used to examine multivariate associations among all the 12 measured functional traits (Table 2) and species were arranged using their scores on the first two principal components. All statistical analysis was made using SAS (v.9.2; SAS institute Inc., Cary, NC, USA).

Results

The three functional groups overall showed significant differences in the three key hydraulic traits, that is, xylem hydraulic efficiency, resistance to drought-induced cavitation and frost fatigue (Fig. 1; Supporting Information Table S1). The RSP species had substantially lower K_s ($1.63\ kg\ m^{-1}\ s^{-1}\ MPa^{-1}$) than the RP group ($4.12\ kg\ m^{-1}\ s^{-1}\ MPa^{-1}$) and NP group ($4.55\ kg\ m^{-1}\ s^{-1}\ MPa^{-1}$, $P < 0.05$, one-way ANOVA; Table S1). The RP species showed significantly higher (less negative) P_{50} values (−1.41 MPa) than the RSP species (−2.51 MPa) and NP species (−2.18 MPa, $P < 0.05$, one-way ANOVA; Table S1). Most notably, both the RSP and RP species showed significantly greater resistance to frost fatigue than the NP species, as indicated by ΔP_{50} values, that is, −0.06 for RSP, −0.09 for RP and −0.31 MPa for NP, respectively ($P < 0.05$, one-way ANOVA; Table S1). Notably, however, one of the species in the RP group (*Alnus japonica*) exhibited considerably more negative ΔP_{50} (−0.33 MPa) than other species of this group (Table S1). The shifts of P_{50} values between the control and the freeze–thaw treated stem segments were evident in the NP group but not in the other two groups (see Figs 2, S1).

Xylem anatomical traits at both the tissue and pit levels varied substantially among the three functional groups (Fig. 3), whereas variations within each of the functional groups were relatively small in most cases (Table S1). The RSP species had significantly lower vessel density ($124.7\ mm^{-2}$) than the RP ($233.5\ mm^{-2}$) and NP species ($362.3\ mm^{-2}$, $P < 0.05$, one-way ANOVA; Table S1). Moreover, the RSP species showed significantly higher vessel solitary index (0.59) than the RP (0.26) and NP species (0.37, $P < 0.05$, one-way ANOVA; Table S1). At the pit level,

Table 2 List of functional traits measured in the present study

Acronym	Definition	Unit
K_s	Specific hydraulic conductivity	$kg\ m^{-1}\ s^{-1}\ MPa^{-1}$
P_{50}	Stem xylem water potential at 50% loss of conductivity	MPa
ΔP_{50}	The difference between the P_{50} of control and freeze–thaw treated stems (less negative values indicate greater resistance to frost fatigue)	MPa
WD	Wood density	$g\ cm^{-3}$
VD	Vessel density	No. mm^{-2}
D	Mean vessel diameter	μm
V_s	Solitary vessel index = number of solitary vessels divided by total number of vessels	–
A_p	Single pit membrane area	μm^2
F_{pf}	Pit-field fraction = fraction of intervessel wall surface occupied by pits	–
A_{ap}	Percentage of total aperture area in unit intervessel wall area	–
F_{ap}	Aperture fraction = pit aperture area/membrane area	–
AP_f	Aperture shape index = ratio of the shortest to the longest axis of the outer pit aperture	–

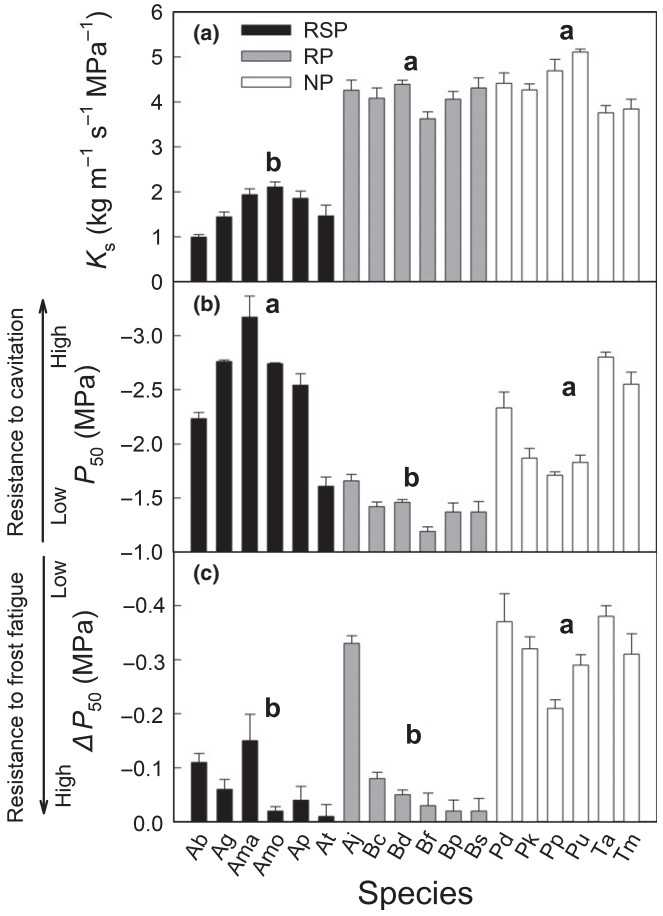

Fig. 1 Mean values for the three key hydraulic traits of the 18 species belonging to the three functional groups. (a) Specific hydraulic conductivity (K_s), (b) stem xylem water potential corresponding to 50% loss of hydraulic conductivity (P_{50}), and (c) the difference between P_{50} of control and freeze–thaw treated stem segments (ΔP_{50}). RSP, species that can generate both stem and root pressures; RP, species that can only generate root pressure; NP, species not being able to generate positive xylem pressure. Error bars show 1 SE ($n = 6$ for K_s and P_{50} and 3 for ΔP_{50}). Different letters above the bars indicate significant differences between groups ($P < 0.05$, one-way ANOVA). Species name abbreviations are as defined in Table 1.

xylem structural traits were dramatically different between the RP species and the other two functional groups (Fig. 3), with RP species having much smaller pit membrane size but higher pit-field fraction and percentage of total aperture area in unit intervessel wall area (Table S1). Most notably, the slit-like pit apertures in the RP species clearly contrast with the oval pit apertures in the other two groups, giving the RP species a significantly lower average AP_f value (0.29) than the RSP (0.44) and NP species (0.67, Table S1). Notably, within the RP group, *Alnus japonica* showed a suite of xylem anatomical trait values that differed from the other five species (Table S1), which is consistent with the finding that this species having a frost fatigue resistance more similar to the NP group (Figs 2, 4j,l).

The correlation analyses between the two different hydraulic safety parameters (P_{50} and ΔP_{50}) and the xylem structural traits indicate that they were determined by structural characteristics at different levels (Table 3), suggesting that resistance to drought-induced cavitation and resistance to frost fatigue are largely independent of each other. However, there were shared traits that show significant correlations with both K_s and one of the two hydraulic safety-related traits, P_{50} and ΔP_{50} (Table 3). Relatively small variation was observed for most of the hydraulic and anatomical traits within each of the three functional groups, as indicated by the clustering of symbols having the same colors (Fig. 4a–l); however, species of different functional groups seem to obey a universal spectrum of xylem structure and function variation (Fig. 4a–l). Across the 18 species of the three different functional groups, K_s correlated positively with vessel density ($P < 0.01$; Fig. 4b) and pit-field fraction ($P < 0.01$; Fig. 4d) and negatively with wood density ($P < 0.05$; Fig. 4a) and solitary vessel index ($P < 0.01$; Fig. 4c). Cavitation resistance was strongly affected by vessel connectivity and pit characteristics, that is, it correlated positively with solitary vessel index ($P < 0.01$; Fig. 4g) but negatively with pit aperture area per unit intervessel wall area ($P < 0.01$; Fig. 4e), pit aperture fraction ($P < 0.01$; Fig. 4f) and pit-field fraction ($P < 0.05$; Fig. 4h). Resistance to frost fatigue was positively correlated with wood density ($P < 0.01$; Fig. 4i) and negatively correlated with vessel density ($P < 0.01$; Fig. 4j), pit area ($P = 0.01$; Fig. 4k) and the index of pit aperture shape ($P < 0.01$; Fig. 4l).

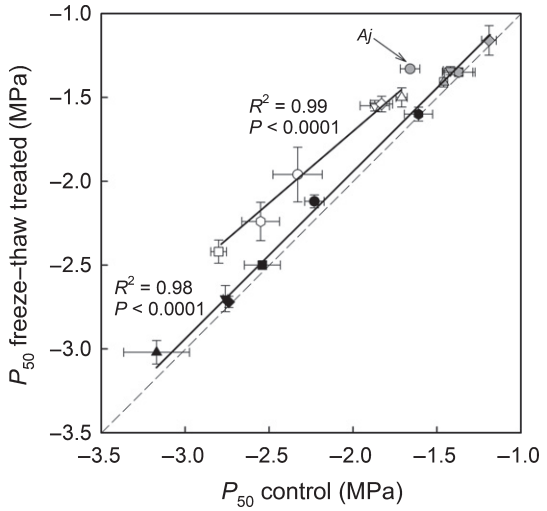

Fig. 2 Mean xylem water potential corresponding to 50% loss of hydraulic conductivity (P_{50}) of the control stems plotted against that of the freeze–thaw treated stems in the 18 studied species. Linear regressions are fitted to the 12 pressure-generating species and the six nonpressure-generating species. The dashed line represents $y = x$. Error bars show ± 1 SE ($n = 3$). Symbols representing each species are as defined in Table 1. The arrow marks *Alnus japonica* (*Aj*), a root pressure-generating species, which deviates obviously from its group.

Across all 18 species, both the resistance to drought-induced cavitation and resistance to frost fatigue showed significant negative correlations with K_s ($P < 0.05$; Fig. 5a,b), whereas no significant correlation was observed between the resistance to frost fatigue and the resistance to drought-induced cavitation ($P = 0.27$; Fig. 5c). At the intragroup level, only two out of the nine possible pairwise correlations among the three key hydraulic traits (K_s, P_{50} and ΔP_{50}) were significant (Fig. S2). Note that the significant correlation between ΔP_{50} and P_{50} across the RP species was driven largely by the divergence of *Alnus japonica* from the other species within this group in hydraulic traits (Fig. S2f), leaving only one meaningful significant correlation at the intragroup level, that is, between P_{50} and K_s across the NP species (Fig. S2g). The lack of overall significant correlations at the intragroup level within the RSP and RP groups is consistent with their relatively small intragroup variation in functional traits, as indicated by the overall tight clustering of the RSP (black symbols) and RP (gray symbols) species along the continuum of trait variations (Fig. 4).

Results of the PCA based on the 12 traits showed that PC1 and PC2 explained 42.9% and 39.1% of the total variation, respectively (Fig. 6a). Functional traits associated with higher hydraulic efficiency but lower resistance to drought-induced cavitation (i.e. K_s, P_{50}, F_{pf}, A_{ap}, F_{ap}) clustered at the positive side of PC axis 1, whereas the trait contributing to stronger resistance to cavitation (i.e. V_s) was loaded at the negative side of PC axis 1 (Fig. 6a). Traits associated with greater resistance to frost fatigue (ΔP_{50}, WD) clustered on the negative side of PC axis 2. By contrast, traits associated with weaker resistance to frost fatigue (VD, A_p, AP_f) were located at the positive side of PC axis 2 (Fig. 6a). Different groups were clearly separated in the space defined by the two PC axes with the RSP group showing greater resistance to cavitation and frost fatigue but lower hydraulic efficiency, the RP group showing greater hydraulic efficiency and resistance to frost fatigue but lower resistance to cavitation, and the NP group showing higher hydraulic efficiency and greater cavitation resistance but lower resistance to frost fatigue (Fig. 6b).

Discussion

Our data support the hypothesis that, in an environment that is strongly affected by freezing stress, tree species differing in the ability to generate positive xylem pressures for winter embolism repair show clear contrasts in a suite of important hydraulic characteristics. Most notably, the two functional groups that generate positive xylem pressures have significantly greater resistance to frost fatigue than the group that does not have this ability, but

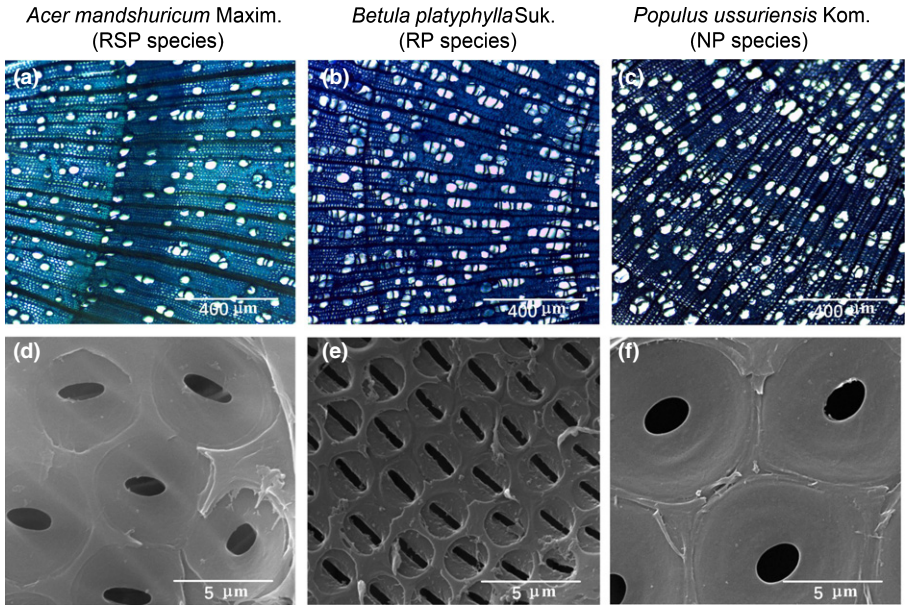

Fig. 3 Images by (a–c) light microscopy and (d–f) scanning electron microscopy for stem xylem of a representative species in each of the three functional groups. RSP, species that can generate both stem and root pressures; RP, species that can only generate root pressure; NP, species not being able to generate positive xylem pressure.

this is at the cost of either reduced hydraulic conductivity or lower resistance to drought-induced cavitation. Our results suggest that divergences in hydraulic properties between functional groups and the hydraulics-related functional trade-offs are underlain by a suite of differences in xylem anatomical characteristics at both the tissue and pit levels.

Divergence in hydraulics and xylem functional trade-offs

Contrasts in xylem hydraulics among the three functional groups, differing in the ability to generate positive xylem pressure and refilling winter-embolized vessels, indicate that freezing played an important role in shaping the divergent adaptive strategies of these sympatric tree species from temperature forests with cold winters (Niu *et al.*, 2017). In the harsh environments of high latitudes and/or high altitudes, freeze–thaw cycles as well as frost drought pose strong stresses on the hydraulic integrity of trees over the winter (Sperry *et al.*, 1994; Mayr *et al.*, 2006; Hao *et al.*, 2013b), which makes the resistances to, or recovery from, freezing- and drought-induced cavitation important for the survival of trees in such environments. Niu *et al.* (2017) showed that the positive-pressure-generating species are effective in refilling winter-embolized vessels resulting in almost complete recovery of hydraulic conductivity in the early growing season. Here, our results further demonstrated that stronger frost fatigue resistance has evolved in the pressure-generating species, which would have important adaptive significance on top of the refilling ability *per se*.

Divergences among functional groups in terms of xylem hydraulics have likely resulted in differences in environmental adaptation and may thus have contributed to niche differentiation along environmental gradients. Besides the strong ability of refilling, species that can generate both root and stem pressures (RSP) show both relatively high resistance to drought-induced cavitation and frost fatigue, but at the cost of decreased hydraulic conductivity compared to the species that can generate root pressure only (RP) and species that do not generate positive xylem pressure (NP) (Fig. 1). The RSP species may benefit from greatly enhanced hydraulic safety in more stressful environments, but the lower hydraulic efficiency may reduce growth and competitiveness under more favorable conditions, considering the strong coordination between hydraulic conductivity and photosynthetic capacity (e.g. Santiago *et al.*, 2004; Hao *et al.*, 2011). Another cost related to the great hydraulic safety of the RSP species is the need to accumulate high concentrations of nonstructural carbohydrates for positive xylem pressure generation, which may compromise structural growth (Sauter *et al.*, 1973; Johnson *et al.*, 1987; Johnson & Tyree, 1992; Cirelli *et al.*, 2008). These physiological characteristics are in agreement with the observation that *Acer* species trees grow relatively slowly and occur only as sub-canopy species in the mixed temperate forests of the Changbai Mountains (Hao *et al.*, 2008b). The RP species show relatively strong frost fatigue resistance (except for *Alnus japonica*) and have conductivity values as high as the NP species, but are considerably less resistant to drought-induced cavitation than both the RSP and NP species (Fig. 1), which implies a lower drought tolerance for RP species. Actually, in the forests at low elevations of the Changbai Mountains, water is usually not a limiting factor, and some *Betula* species are fast-growing and often exist as co-dominant species (Hao *et al.*, 2008b). The NP species would benefit from relatively high hydraulic conductivity and resistance to drought but would have a disadvantage in harsher environments with high risks of winter embolism, contributing to an overall weaker frost resistance than *Acer* and *Betula* species, that is, two groups of species well-known for tolerating extremely low temperatures (Sakai, 1978). The obvious divergences in xylem hydraulics observed here between these functional groups may provide an important basis for species niche differentiation and co-existence in the heterogeneous environments (Hao *et al.*, 2008a, 2013a; Taneda & Sperry, 2008; Christoffersen *et al.*, 2017; Cosme *et al.*, 2017; Zhang *et al.*, 2017).

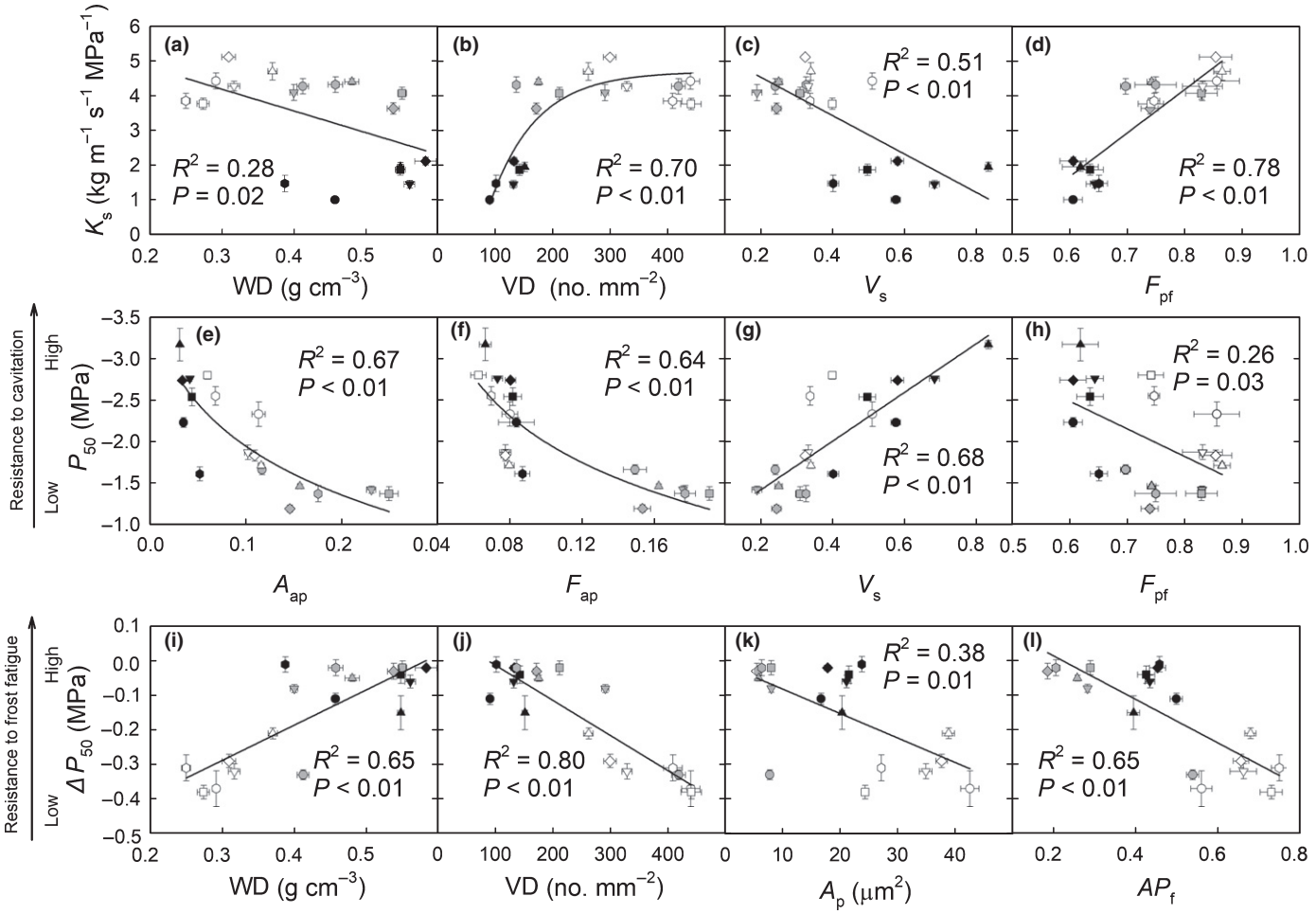

Fig. 4 Correlations between the three key stem hydraulic traits with sapwood structural characteristics across the 18 studied species. The relationships between specific hydraulic conductivity (K_s) and (a) wood density (WD), (b) vessel density (VD), (c) solitary vessel index (V_s), (d) pit-field fraction (F_{pf}); The relationships between stem xylem water potential corresponding to 50% loss of hydraulic conductivity (P_{50}) and (e) percentage of total aperture area in unit intervessel wall area (A_{ap}), (f) aperture fraction (F_{ap}), (g) V_s, and (h) F_{pf}. The relationships between the difference between P_{50} of control and freeze–thaw treated stem segments (ΔP_{50}) and (i) WD, (j) VD, (k) single pit membrane area (A_p), and (l) aperture shape index (AP_f). Please note the inverted direction of the axis scaling for P_{50} in (e–h). Error bars show ± 1 SE (n = 3 for ΔP_{50} and 6 for all other traits). Linear regression or exponential functions are fitted to the data in each panel.

Table 3 Pearson correlation coefficients between the three key hydraulic traits (K_s, P_{50}, ΔP_{50}) and wood anatomical characteristics (acronyms as given in Table 2) across the 18 studied species

	K_s		P_{50}		ΔP_{50}	
	r	P	r	P	r	P
WD	**−0.52**	**0.025**	−0.03	0.90	**0.81**	**< 0.001**
VD	**0.65**	**< 0.01**	−0.06	0.82	**−0.90**	**< 0.001**
D	−0.46	0.054	−0.39	0.11	0.36	0.141
V_s	**−0.72**	**< 0.01**	**−0.83**	**< 0.001**	0.09	0.709
A_p	0.14	0.589	−0.38	0.113	**−0.62**	**< 0.01**
F_{pf}	**0.87**	**< 0.001**	**0.51**	**0.031**	0.43	0.076
A_{ap}	**0.67**	**< 0.01**	**0.79**	**< 0.001**	0.17	0.511
F_{ap}	0.38	0.118	**0.82**	**< 0.001**	0.44	0.065
AP_f	0.15	0.566	−0.45	0.059	**−0.81**	**< 0.001**

Bold values indicate significant correlations (P < 0.05). Correlations with P < 0.05 are shown with a gray background.

The divergence in xylem hydraulics between the three functional groups seems to involve multiple trade-offs of xylem functioning, reflecting antagonistic xylem structural requirements at both the tissue and pit levels in fulfilling different functions, that is, conductivity, resistance to drought and frost fatigue (Fig. 4a–l). For example, higher degrees of vessel interconnectivity (lower solitary vessel index, V_s) resulting in higher maximum specific hydraulic conductivity (K_s) in RP and NP species (Fig. 4c), by allowing water to move more freely between conduits, unavoidably results in greater susceptibility to drought-induced embolism in these two groups (Fig. 4g), because greater connectivity also makes embolism more easily expand between neighboring vessels through air seeding (Loepfe *et al.*, 2007; Scholz *et al.*, 2013). Our data strongly indicate that all of the species are in line with the uniform multidimensional structure–function relationships, irrespective of their ability in positive pressure generation (Fig. 4), which leads to significant trade-offs across the 18 studied species

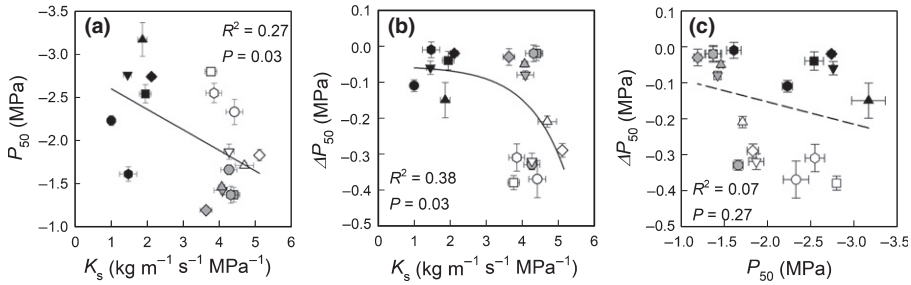

Fig. 5 Correlations among the three key hydraulic traits across the 18 studied species belonging to the three functional groups. K_s, specific hydraulic conductivity; P_{50}, stem xylem water potential corresponding to 50% loss of hydraulic conductivity; ΔP_{50}, the difference between P_{50} of control and freeze–thaw treated stem segments. Error bars show ± 1 SE ($n = 6$ for K_s and P_{50} and 3 for ΔP_{50}). (a, c) Linear regression or (b) exponential functions are fitted to the data. Color-coding for functional groups and symbol definition for each species are as shown in Table 1.

between resistance to drought-induced cavitation and K_s (Fig. 5a), as well as between frost fatigue resistance and K_s (Fig. 5b). However, largely due to the relatively small trait variation within each of the three functional groups, no meaningful significant correlation was found among the three key hydraulic traits at the intragroup level, except the one between xylem water potential corresponding to 50% loss of hydraulic conductivity (P_{50}) and K_s in the NP species group (Fig. S2g).

Different structural requirements for cavitation and frost fatigue resistances

Our results suggest that xylem resistance to drought-induced cavitation and to frost fatigue are determined by different structural characteristics at both the tissue and pit levels, and that cavitation resistance and frost fatigue resistance are therefore decoupled (Fig. 5c). In general, resistance to drought-induced cavitation is associated mainly with the spatial distribution of the vessel network and the area fractions of the pit membrane and apertures (Fig. 4e–h). Our findings in the correlation between P_{50} and vessel connectivity across the 18 species are in agreement with the hydraulic model optimized by Martínez-vilalta *et al.* (2012) based on data of 97 species. Species with greater resistance to drought-induced cavitation had more solitary vessels, whereas species that are more sensitive to cavitation often exhibit high degrees of vessel interconnectivity resulting in easier spreading of embolism by air seeding through intervessel pits (Loepfe *et al.*, 2007; Scholz *et al.*, 2013). Consistent with previous studies, larger pit membrane area per unit intervessel wall area also is associated with lower resistance to cavitation (Hacke *et al.*, 2006; Lens *et al.*, 2011), which is in line with the 'rare pit' hypothesis for the formation and spreading of embolism under drought stress, that is, with the increase of pit membrane area per unit intervessel wall area the probability that a vessel contains a 'leakier' pit for air seeding and thus lowered threshold for cavitation would increase (Christman *et al.*, 2009). In addition, it has been found that pit aperture that occupies a smaller proportion of the pit border (smaller aperture fraction, F_{ap}) contributes to the minimization of the mechanical damage on the aspirated pit membrane during drought stress and hence increased cavitation resistance (Lens *et al.*, 2011). For example, a combination of relatively low vessel solitary index and higher aperture fraction contribute to

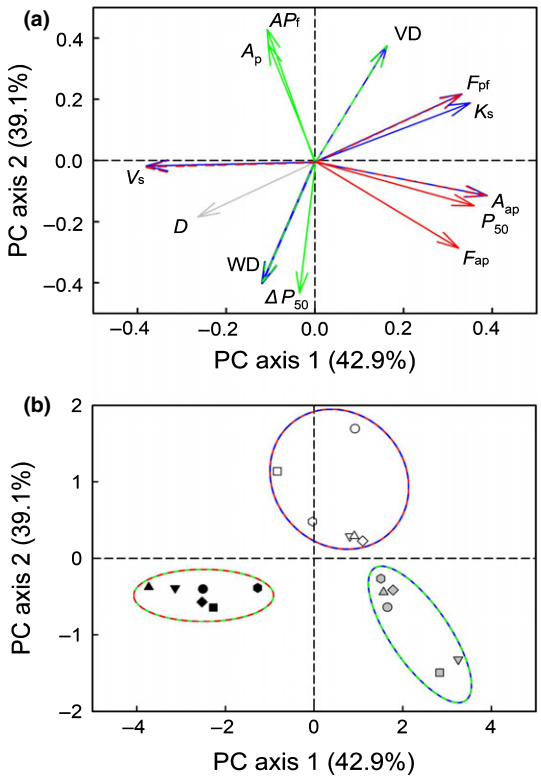

Fig. 6 Results of the principal component (PC) analysis of the 18 species using the 12 measured functional traits. (a) The 12 functional traits arranged along the first two PC axes, and (b) the 18 studied species loaded in the space defined by PC axis 1 and PC axis 2, showing the separation of the three functional groups. In (a), the blue, red and green arrows indicate K_s, P_{50} and ΔP_{50} as well as traits having significant correlations with each of them as shown in Table 3. Dashed arrows that consist of two colors represent correlations with two of the key hydraulic traits. The gray arrow indicates that D does not have significant correlation with any of the hydraulic traits. In (b), the two colors for each ellipse indicate the association of each group with two of the three key hydraulic traits, that is, greater hydraulic efficiency (blue), stronger resistance to cavitation (red) and resistance to frost fatigue (green). Symbols representing each species and trait name abbreviations are as defined in Tables 1 and 2.

significantly lower cavitation resistance in the RP species relative to the other two functional groups (Fig. 1; Table S1).

Different from the resistance to drought-induced cavitation, frost fatigue resistance is associated mainly with wood density,

vessel density and single pit characteristics (Fig. 4i–l). Wood density has been used as an integrative proxy for mechanical reinforcement that contributes to enhanced resistance to conduit implosions under strong negative pressures due to its direct relationship with the double-wall thickness relative to vessel lumen diameter (Hacke *et al.*, 2001a; Jacobsen *et al.*, 2005). Significantly higher wood densities in the RSP and RP species compared with those of the NP species may thus have contributed to enhanced ability of their vessels in withstanding xylem stretching during the process of freezing because the ice nucleation can result in volume expansions of the vessel lumens (Milburn & O'Malley, 1984; Cavender-Bares, 2005). In diffuse-porous species, the increase in vessel density is usually compensated by a decreased fiber frequency and lower wood density (Jacobsen *et al.*, 2007), which leads to an indirect correlation between vessel density and frost fatigue resistance across the 18 studied species (Fig. 4j). Moreover, resistance to frost fatigue is apparently associated with reduced damage risks to xylem pit structures during the process of extracellular freezing. When ice forms in the extracellular space, it creates a water potential gradient and draws water from neighboring cells due to the growth of ice crystals and upon thawing the cells can soon reabsorb water if they have not been injured during freezing (Meryman, 1968; Sakai & Larcher, 1987). Extracellular freezing is largely innocuous to cells (Sakai & Otsuka, 1967; Sakai & Yoshida, 1967); however, the growth of ice crystals during extracellular freezing might stretch the pit membrane and loose the cellulosic mesh and, finally, induce frost fatigue (Hacke *et al.*, 2006). It has been proven that smaller pit size is usually associated with thicker pit membrane and lower pit membrane porosity (Sperry & Hacke, 2004). In the RSP and RP species, smaller pit membrane sizes, and hence thicker pit membranes, have likely contributed to the protection of pore expansion and rupture of the pit membrane during the process of extracellular freezing (Christman *et al.*, 2009). Moreover, in analogy to the role of minimizing mechanical damage to the aspirated pit membrane during drought stress (Lens *et al.*, 2011), the smaller and more slit-like apertures in RSP and particularly in RP species would minimize mechanical damage during extracellular ice nucleation and thus contribute to their greater frost fatigue resistance than the NP species.

Concluding remarks

Our results demonstrate that stronger resistance to frost fatigue has evolved in temperate tree species that refill winter-embolized vessels using positive xylem pressures compared to species that cannot generate such pressures. Resistances to frost fatigue and drought-induced xylem embolism are two key hydraulic characteristics largely independent of each other due to the fact that they are determined by different xylem structural characteristics at both the tissue and pit levels. Moreover, differences in the form of positive xylem pressure generation in representative tree species also resulted in substantial divergence in their hydraulic architecture, including hydraulic conductivity and resistance to drought-induced cavitation. The divergences in hydraulic architecture among these functional groups with different strategies of coping with winter embolism, as reflected by multifaceted trade-offs in xylem design, may have contributed to species co-existence under a typical temperate climate condition where freezing poses a strong threat to the hydraulic integrity of trees.

Acknowledgements

The staff at the Research Station of Changbai Mountain Forest Ecosystems and other members of Dr Hao's lab are gratefully acknowledged for supporting this study. We are grateful to Professors Melvin Tyree and Yujie Wang for help with the Cavitron technique. This work was supported by the National Natural Science Foundation of China (31722013, 31500222), the National Key Research and Development Program of China (2016YFA0600803), the Hundred-Talents Program and the project QYZDJ-SSW-DQC027 from the Chinese Academy of Sciences and the Royal Netherlands Academy of Arts and Sciences (China Exchange Program Project 530-5CDP20). All data used in this manuscript are presented in the manuscript and the supporting information. The authors declare no conflict of interests.

Author contributions

G.Y.H. and X.H.Y. designed the study; X.H.Y. conducted field and laboratory measurements; X.H.Y., G.Y.H. and F.S. analyzed and interpreted the data; G.Y.H. and X.H.Y. wrote the manuscript that was edited intensively by all authors.

ORCID

Guang-You Hao http://orcid.org/0000-0002-6003-7003

References

Améglio T, Bodet C, Lacointe A, Cochard H. 2002. Winter embolism, mechanisms of xylem hydraulic conductivity recovery and springtime growth patterns in walnut and peach trees. *Tree Physiology* **22**: 1211–1220.

Améglio T, Decourteix M, Alves G, Valentin V, Sakr S, Julien JL, Petel G, Guilliot A, Lacointe A. 2004. Temperature effects on xylem sap osmolarity in walnut trees: evidence for a vitalistic model of winter embolism repair. *Tree Physiology* **24**: 785–793.

Cai J, Tyree MT. 2010. The impact of vessel size on vulnerability curves: data and models for within-species variability in saplings of aspen, *Populus tremuloides* Michx. *Plant, Cell & Environment* **33**: 1059–1069.

Cavender-Bares J. 2005. Impacts of freezing on long distance transport in woody plants. In: Holbrook NM, Zweiniecki MA, eds. *Vascular transport in plants.* Amsterdam, the Netherlands: Academic Press, 401–424.

Charra-Vaskou K, Badel E, Charrier G, Ponomarenko A, Bonhomme M, Foucat L, Mayr S, Améglio T. 2016. Cavitation and water fluxes driven by ice water potential in *Juglans regia* during freeze–thaw cycles. *Journal of Experimental Botany* **67**: 739–750.

Chave J, Coomes D, Jansen S, Lewis SL, Swenson NG, Zanne AE. 2009. Towards a worldwide wood economics spectrum. *Ecology Letters* **12**: 351–366.

Choat B, Medek DE, Stuart SA, Pasquet-Kok J, Egerton JJG, Salari H. 2011. Xylem traits mediate a trade-off between resistance to freeze–thaw-induced

embolism and photosynthetic capacity in overwintering evergreens. *New Phytologist* **191**: 996–1005.

Christensen-Dalsgaard KK, Tyree MT. 2013. Does freezing and dynamic flexing of frozen branches impact the cavitation resistance of *Malus domestica* and the *Populus* clone Walker? *Oecologia* **173**: 665–674.

Christensen-Dalsgaard KK, Tyree MT. 2014. Frost fatigue and spring recovery of xylem vessels in three diffuse-porous trees *in situ*. *Plant, Cell & Environment* **37**: 1074–1085.

Christman MA, Sperry JS, Adler FR. 2009. Testing the 'rare pit' hypothesis for xylem cavitation resistance in three species of *Acer*. *New Phytologist* **182**: 664–674.

Christman MA, Sperry JS, Smith DD. 2012. Rare pits, large vessels and extreme vulnerability to cavitation in a ring-porous tree species. *New Phytologist* **193**: 713–720.

Christoffersen B, Meir P, Mcdowell NG. 2017. Linking plant hydraulics and beta diversity in tropical forests. *New Phytologist* **215**: 12–14.

Cirelli D, Jagels D, Tyree MT. 2008. Toward an improved model of maple sap exudation: the location and role of osmotic barriers in sugar maple, butternut and white birch. *Tree Physiology* **28**: 1145–1155.

Cochard H, Damour G, Bodet C, Tharwat I, Poirier M, Améglio T. 2005. Evaluation of a new centrifuge technique for rapid generation of xylem vulnerability curves. *Physiologia Plantarum* **124**: 410–418.

Cochard H, Herbette S, Barigah T, Badel E, Ennajeh M, Vilagrosa A. 2010. Does sample length influence the shape of xylem embolism vulnerability curves? A test with the cavitron spinning technique. *Plant, Cell & Environment* **33**: 1543–1552.

Cochard H, Tyree MT. 1990. Xylem dysfunction in *Quercus*: vessel sizes, tyloses, cavitation and seasonal changes in embolism. *Tree Physiology* **6**: 393–407.

Cosme LHM, Schietti J, Costa FRC, Oliveira RS. 2017. The importance of hydraulic architecture to the distribution patterns of trees in a central Amazonian forest. *New Phytologist* **215**: 113–125.

Davis SD, Sperry JS, Hacke UG. 1999. The relationship between xylem conduit diameter and cavitation caused by freezing. *American Journal of Botany* **86**: 1367–1372.

Ewers FW, Améglio T, Cochard H, Beaujard F, Martignac M, Vandame M, Bodet C, Cruiziat C. 2001. Seasonal variation in xylem pressure of walnut trees: root and stem pressures. *Tree Physiology* **21**: 1123–1132.

Feild TS, Brodribb T. 2001. Stem water transport and freeze–thaw xylem embolism in conifers and angiosperms in a Tasmanian treeline heath. *Oecologia* **127**: 314–320.

Feng F, Ding F, Tyree MT. 2015. Investigations concerning cavitation- and frost-fatigue in clonal *Populus* 84k using 'high resolution' cavitron measurements. *Plant Physiology* **168**: 144–155.

Granda E, Scoffoni C, Rubio-Casal AE, Sack L, Valladares F. 2014. Leaf and stem physiological responses to summer and winter extremes of woody species across temperate ecosystems. *Oikos* **123**: 1281–1290.

Hacke UG, Sauter JJ. 1996. Xylem dysfunction during winter and recovery of hydraulic conductivity in diffuse-porous and ring-porous trees. *Oecologia* **105**: 435–439.

Hacke UG, Sperry JS. 2001. Functional and ecological xylem anatomy. *Perspectives in Plant Ecology Evolution and Systematics* **4**: 97–115.

Hacke UG, Sperry JS, Pockman WT, Davis SD, McCulloh KA. 2001a. Trends in wood density and structure are linked to prevention of xylem implosion by negative pressure. *Oecologia* **126**: 457–461.

Hacke UG, Sperry JS, Wheeler JK, Castro L. 2006. Scaling of angiosperm xylem structure with safety and efficiency. *Tree Physiology* **26**: 689–701.

Hacke UG, Stiller V, Sperry JS, Pittermann J, Mcculloh KA. 2001b. Cavitation fatigue. embolism and refilling cycles can weaken the cavitation resistance of xylem. *Plant Physiology* **125**: 779–786.

Hao GY, Goldstein G, Sack L, Holbrook NM, Liu ZH, Wang AY, Harrison RD, Su ZH, Cao KF. 2011. Ecology of hemiepiphytism in fig species is based on evolutionary correlation of hydraulics and carbon economy. *Ecology* **92**: 2117–2130.

Hao GY, Hoffmann WA, Scholz FG, Bucci SJ, Meinzer FC, Franco AC. 2008a. Stem and leaf hydraulics of congeneric tree species from adjacent tropical savanna and forest ecosystems. *Oecologia* **155**: 405–415.

Hao ZQ, Li BH, Zhang J, Wang XG, Ye J. 2008b. Broad-leaved Korean pine (*Pinus koraiensis*) mixed forest plot in Changbaishan (CBS) of China: community composition and structure. *Journal of Plant Ecology* **32**: 238–250.

Hao GY, Lucero ME, Sanderson SC, Zacharias EH, Holbrook NM. 2013a. Polyploidy enhances the occupation of heterogeneous environments through hydraulic related trade-offs in *Atriplex canescens* (Chenopodiaceae). *New Phytologist* **197**: 970–978.

Hao GY, Wheeler JK, Michele HN, Guillermo G. 2013b. Investigating xylem embolism formation, refilling and water storage in tree trunks using frequency domain reflectometry. *Journal of Experimental Botany* **64**: 2321–2332.

Jacobsen AL, Ewers FW, Pratt RB, Paddock WA, Davis SD. 2005. Do xylem fibers affect vessel cavitation resistance? *Plant Physiology* **139**: 546–556.

Jacobsen AL, Pratt RB, Ewers FW, Davis SD. 2007. Cavitation resistance among 26 chaparral species of southern California. *Ecological Monographs* **77**: 99–115.

Jiménez-Castillo M, Lusk CH. 2013. Vascular performance of woody plants in a temperate rain forest: lianas suffer higher levels of freeze–thaw embolism than associated trees. *Functional Ecology* **27**: 403–412.

Johnson RW, Tyree MT. 1992. Effect of stem water content on sap flow from dormant maple and butternut stems. *Plant Physiology* **100**: 853–858.

Johnson RW, Tyree MT, Dixon MA. 1987. A requirement for sucrose in xylem sap flow from dormant maple trees. *Plant Physiology* **84**: 495–500.

Kitin P, Funada R. 2016. Earlywood vessels in ring-porous trees become functional for water transport after bud burst and before the maturation of the current-year leaves. *IAWA Journal* **37**: 315–331.

Lemoine D, Granier A, Cochard H. 1999. Mechanism of freeze-induced embolism in *Fagus sylvatica* L. *Trees* **13**: 206–210.

Lens F, Sperry JS, Christman MA, Choat B, Rabaey D, Jansen S. 2011. Testing hypotheses that link wood anatomy to cavitation resistance and hydraulic conductivity in the genus *Acer*. *New Phytologist* **190**: 709–723.

Lens F, Tixier A, Cochard H, Sperry JS, Jansen S, Herbette S. 2013. Embolism resistance as a key mechanism to understand adaptive plant strategies. *Current Opinion in Plant Biology* **16**: 287–292.

Loepfe L, Martinez-Vilalta J, Piñol J, Mencuccini M. 2007. The relevance of xylem network structure for plant hydraulic efficiency and safety. *Journal of Theoretical Biology* **247**: 788–803.

Martínez-vilalta J, Mencuccini M, Alvarez X, Camacho J, Loepfe L, Piñol J. 2012. Spatial distribution and packing of xylem conduits. *American Journal of Botany* **99**: 1189–1196.

Mayr S, Hacke U, Schmid P, Schwienbacher F, Gruber A. 2006. Frost drought in conifers at the alpine timberline: xylem dysfunction and adaptations. *Ecology* **87**: 3175–3185.

Mayr S, Wolfschwenger M, Bauer H. 2002. Winter-drought induced embolism in norway spruce (*Picea abies*) at the alpine timberline. *Physiologia Plantarum* **115**: 74–80.

Meryman HT. 1968. Observations on the present state of blood preservation by freezing. *Cryobiology* **5**: 144–146.

Milburn JA, O'Malley PER. 1984. Freeze-induced sap absorption in *Acer pseudoplatanus*: a possible mechanism. *Canadian Journal of Botany* **62**: 2101–2106.

Niu CY, Meinzer FC, Hao GY. 2017. Divergence in strategies for coping with winter embolism among co-occurring temperate tree species: the role of positive xylem pressure, wood type and tree stature. *Functional Ecology* **35**: 1550–1560.

Pittermann J, Sperry JS. 2006. Analysis of freeze–thaw embolism in conifers. The interaction between cavitation pressure and tracheid size. *Plant Physiology* **140**: 374–382.

Pockman WT, Sperry JS. 1996. Freezing-induced xylem cavitation and the northern limit of *Larrea tridentata*. *Oecologia* **109**: 19–27.

Reich PB. 2014. The world-wide fast-slow plant economics spectrum: a traits manifesto. *Journal of Ecology* **102**: 275–301.

Sakai A. 1978. Freezing tolerance of evergreen and deciduous broad-leaved trees in Japan with reference to tree regions. *Low Temperature Science, Series B* **36**: 1–19.

Sakai A, Larcher W. 1987. Frost survival of plants. *Ecological Studies* **62**: 104–127.

Sakai A, Otsuka K. 1967. Survival of plant tissue at super-low temperatures V. An electron microscope study of ice in cortical cells cooled rapidly. *Plant Physiology* **42**: 1680–1694.

Sakai A, Yoshida S. 1967. Survival of plant tissue at super-low temperature VI. Effects of cooling and rewarming rates on survival. *Plant Physiology* **42**: 1695–1701.

Santiago LS, Kitajima K, Wright SJ, Mulkey SS. 2004. Coordinated changes in photosynthesis, water relations and leaf nutritional traits of canopy trees along a precipitation gradient in lowland tropical forest. *Oecologia* **139**: 495–502.

Sauter JJ, Iten W, Zimmermann MH. 1973. Studies on the release of sugar into the vessels of sugar maple (*Acer saccharum*). *Canadian Journal of Botany* **51**: 1–8.

Scholz A, Rabaey D, Stein A, Cochard H, Smets E, Jansen S. 2013. The evolution and function of vessel and pit characters with respect to cavitation resistance across 10 *Prunus* species. *Tree Physiology* **33**: 684–694.

Schreiber SG, Hamann A, Hacke UG, Thomas BR. 2013. Sixteen years of winter stress: an assessment of cold hardiness, growth performance and survival of hybrid poplar clones at a boreal planting site. *Plant, Cell & Environment* **36**: 419–428.

Sperry JS. 1993. Winter xylem embolism and spring recovery in *Betula cordifolia*, *Fagus grandifolia*, *Abies balsamea* and *Picea rubens*. In: Raschi A, Borghetti M, Grace J, eds. *Water transport in plants under climatic stress*. Cambridge, UK: Cambridge University Press, 86–98.

Sperry JS, Donnelly JR, Tyree MT. 1988a. A method for measuring hydraulic conductivity and embolism in xylem. *Plant, Cell & Environment* **11**: 35–40.

Sperry JS, Donnelly JR, Tyree MT. 1988b. Seasonal occurrence of xylem embolism in sugar maple (*Acer saccharum*). *American Journal of Botany* **75**: 1212–1218.

Sperry JS, Hacke UG. 2004. Analysis of circular bordered pit function I. angiosperm vessels with homogenous pit membranes. *American Journal of Botany* **91**: 369–385.

Sperry JS, Holbrook NM, Zimmermann MH, Tyree MT. 1987. Spring filling of xylem vessels in wild grapevine. *Plant Physiology* **83**: 414–417.

Sperry JS, Nichols KL, Sullivan JEM, Eastlack SE. 1994. Xylem embolism in ring-porous, diffuse-porous, and coniferous trees of northern Utah and interior Alaska. *Ecology* **75**: 1736–1752.

Sperry JS, Sullivan JE. 1992. Xylem embolism in response to freeze–thaw cycles and water stress in ring-porous, diffuse-porous, and conifer species. *Plant Physiology* **100**: 605–613.

Stiller V, Sperry JS. 2002. Cavitation fatigue and its reversal in sunflower (*Helianthus annuus* L.). *Journal of Experimental Botany* **53**: 1155–1161.

Taneda H, Sperry JS. 2008. A case-study of water transport in co-occurring ring-versus diffuse-porous trees: contrasts in water-status, conducting capacity, cavitation and vessel refilling. *Tree Physiology* **28**: 1641–1651.

Tibbetts TJ, Ewers FW. 2000. Root pressure and specific conductivity in temperate lianas: exotic *Celastrus orbiculatus* (Celastraceae) vs. native *Vitis riparia* (Vitaceae). *American Journal of Botany* **87**: 1272–1278.

Tyree MT. 1983. Maple sap uptake, exudation and pressure changes correlated with freezing exotherms and thawing endotherms. *Plant Physiology* **73**: 277–285.

Tyree MT, Sperry JS. 1989. Vulnerability of xylem cavitation and embolism. *Annual Review of Plant Biology* **40**: 19–38.

Tyree MT, Yang S. 1992. Hydraulic conductivity recovery versus water pressure in xylem of *Acer saccharum*. *Plant Physiology* **100**: 669–676.

Wheeler JK, Sperry JS, Hacke UG, Hoang N. 2005. Intervessel pitting and cavitation in woody Rosaceae and other vesselled plants: a basis for a safety versus efficiency trade-off in xylem transport. *Plant, Cell & Environment* **28**: 800–812.

Zhang WW, Song J, Wang M, Liu YY, Li N, Zhang YJ, Holbrook NM, Hao GY. 2017. Divergences in hydraulic architecture form an important basis for niche differentiation between diploid and polyploid *Betula* species in NE China. *Tree Physiology* **34**: 604–616.

Zimmermann MH. 1983. *Xylem structure and the ascent of sap*. Berlin, Germany: Springer.

Supporting Information

Additional Supporting Information may be found online in the Supporting Information tab for this article:

Fig. S1 Changes in the percentage loss of conductivity in relation to xylem pressure generated by centrifugal force for the 18 studied species belong to the three groups.

Fig. S2 Correlations among the three key hydraulic functional traits (K_s, P_{50} and ΔP_{50}) within each of the three functional groups.

Table S1 Stem hydraulics-related traits of the 18 studied species belonging to the three functional groups

Please note: Wiley Blackwell are not responsible for the content or functionality of any Supporting Information supplied by the authors. Any queries (other than missing material) should be directed to the *New Phytologist* Central Office.